Vol 11 No 10, October 2002
1009-1963/2002/11(10)/1022-06

Chinese Physics

© 2002 Chin. Phys. Soc.
and IOP Publishing Ltd

A virtual optical probe based on evanescent wave interference*

Sun Li-Qun(孙利群)†, Wang Jia(王 佳),
Hong Tao(洪 涛), and Tian Qian(田 芊)

Department of Precision Instruments, State Key Laboratory of Precision Measurement Technology and Instruments, Tsinghua University, Beijing 100084, *China*

(Received 28 January 2002; revised manuscript received 23 April 2002)

A virtual probe is a novel immaterial tip based on the near-field evanescent wave interference and small aperture diffraction, which can be used in near-field high-density optical data storage, nano-lithography, near-field optical imaging and spectral detection, near-field optical manipulation of nano-scale specimen, etc. In this paper, the formation mechanism of the virtual probe is analysed, the evanescent wave interference discussed theoretically, and the sidelobe suppression by small aperture is simulated by the three-dimensional finite-difference time-domain method. The simulation results of the optical distribution of the near-field virtual probe reveal that the transmission efficiency of the virtual probe is 10^2–10^4 times higher than that of the nano-aperture metal-coated fibre probe widely used in near-field optical systems. The full width at half maximum of the peak, in other words, the size of virtual probe, is constant whatever the distance in a certain range so that the critical nano-separation control in the near-field system can be relaxed. We give an example of the application of the virtual probe in ultrahigh-density optical data storage.

Keywords: near-field optics, evanescent wave interference, virtual probe, finite-difference time-domain method

PACC: 4225, 4290

1. Introduction

In recent years, scanning near-field optical microscopy (SNOM) has stimulated continuous research interest as it can provide an efficient way to obtain the optical information of surface structure with a sub-wavelength resolution.[1–4] These novel devices have been applied in a wide range of physics, surface chemistry, material science and biology, such as the detection of topography, spectroscopy, as well as high-density information storage.

The optical probe is the most essential component governing the performance of SNOM. The resolution of SNOM is determined by the size of the probe tip, and the response sensitivity by its output intensity. Several kinds of probes are widely used in near-field optical technology, such as fibre probes, apertureless probes, plasmon probes, etc.[5] But there are some shortcomings in these probes. Low transmission efficiency, slow feedback rate due to rigorous distance control, and fragility of the probe restrict the development of probe-type near-field optical systems.

To overcome the drawbacks of real probes, the concept of an immaterial probe was first proposed by Grosjean and Courjon in 2001.[6] A confined light distribution is generated due to the evanescent wave interference. The confinement distribution peak, called the virtual probe, is independent of the distance z. This new concept can be used in SNOM and other near-field optical systems, allowing the scanning of a sample without any mechanical contact with it. It will be a good challenge to confocal microscopy.

Because the virtual probe concept was proposed just a few months ago, its formation mechanism and characteristics have not been discussed clearly. In this paper, the evanescent wave interference is studied theoretically, the sidelobe suppression by a small aperture is simulated by the three-dimensional finite-difference time-domain (FDTD) method, and the formation mechanism of the virtual probe is analysed. We give an example of the application of the virtual probe in ultrahigh-density optical data storage.

*Project supported by the State Key Development Programme for Basic Research of China (Grant No G1999033002), by the Tsinghua University 985 Foundation for Optical Information Storage (the Subproject of Near-field Optical Storage) and by the China Postdoctoral Science Foundation.

†E-mail: sunlq@pim.tsinghua.edu.cn

2. Evanescent wave interference

When light is propagated from an optically dense medium (with refractive index n_1) into one which is optically less dense (with refractive index n_2, $n_2 < n_1$), the light suffers total reflection provided that the angle of incidence θ_i exceeds the critical angle θ_c given by $\theta_c = n_2/n_1$. Light beyond the critical angle has the interesting property that it effectively passes into the less dense medium a small distance before it is reflected[7] (see Fig.1). In the less dense medium, there is an evanescent wave which is propagated along the interface in the plane of incidence (i.e. in the positive x-direction), and which decays exponentially with the distance z from the interface. In the Cartesian coordinate system shown in Fig.1, the refractive wave can be written as[8]

$$E_2 = A\mathrm{e}^{-k_1 z\sqrt{\sin^2\theta_i - n^2}}\mathrm{e}^{-\mathrm{i}(\omega t - k_1 x\sin\theta_i)}, \qquad (1)$$

where A is the amplitude of the wave, $k_1 = n_1\omega/c = 2\pi n_1/\lambda$ are the wavenumbers in medium 1, ω is the angular frequency, λ is the wavelength in vacuum, and $n = n_2/n_1$ is the relative refractive index.

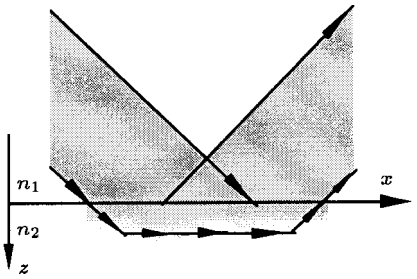


Fig.1. An illustration of the total reflection and evanescent wave.

If another wave incidences in the output direction of the reflection wave of the previous incident light, in the less dense medium there is another evanescent wave which is propagated along the interface in the opposite direction ($-x$-direction). On the assumption that the intensity of the two incident lights is the same, the second evanescent wave can be expressed as

$$E_2' = A\mathrm{e}^{-k_1 z\sqrt{\sin^2\theta_i - n^2}}\mathrm{e}^{-\mathrm{i}(\omega t + k_1 x\sin\theta_i)}). \qquad (2)$$

In the overlap area, interference occurs between two evanescent waves (see Fig.2). The interference field intensity distribution is

$$I = 2A^2\mathrm{e}^{-2k_1 z\sqrt{\sin^2\theta_i - n^2}}\left[1 + \cos\left(\frac{4\pi n_1 x}{\lambda}\sin\theta_i\right)\right]. \qquad (3)$$

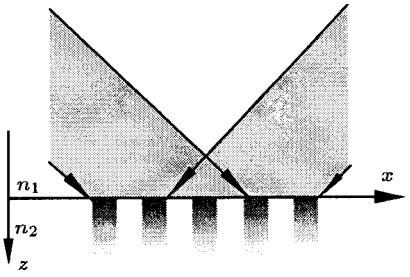


Fig.2. An illustration of the evanescent wave interference.

This shows that the spatial period of the interference fringe is $\lambda/2n_1\sin\theta_i$, the peak intensity of every fringe $4A^2\mathrm{e}^{-2k_1 z\sqrt{\sin^2\theta_i - n^2}}$ at some observation plane, and the full width at half maximum (FWHM) $\lambda/4n_1\sin\theta_i$, with λ=650nm, n_1=2, n_2=1, $\theta_i = 45°$, FWHM=115nm.

To understand clearly the formation of the interference pattern, the propagation process of two plane waves incident with angles larger than θ_c is simulated numerically by the three-dimensional FDTD method.[9] Numerical calculation by the FDTD method is the most popular and promising method for this purpose,[10,11] because it can be easily applied to actual three-dimensional problems. The FDTD method is based on the two Maxwell curl equations in derivative form in the time domain, of which the reliability has been confirmed by the agreement of simulation results with experiment in many researches.[12]

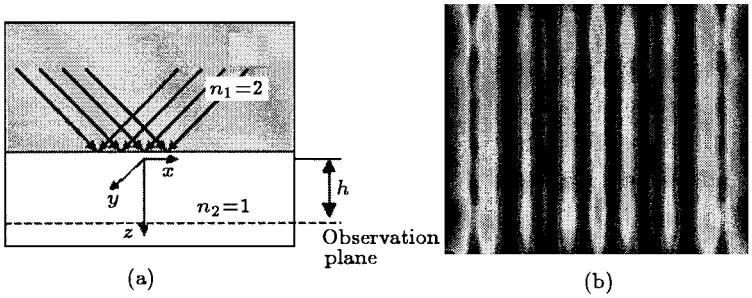


Fig.3. (a) Evanescent wave interference simulation model. (b) Interference pattern in the observation plane (h=250nm).

Fig.3(a) shows the simulation model. The Cartesian coordinate origin is set in the centre of the interface. The whole simulation space is divided into 10^3 equal discrete units, each of which has the volume of $\Delta x \Delta y \Delta z$, where Δx, Δy, Δz are all 50nm. The wavelength of the incident light is 650nm and the polarization direction is y. The distance between the observation plane and the interface is h. The refractive indices of two media are 2 and 1, respectively. The incident angle is 45° to generate the total internal reflection.

Fig.3(b) shows the interference pattern in the observation plane (h=250nm). It reveals that the evanescent wave exists in the vicinity of the interface due to total reflection and the interference fringes are produced by the evanescent wave interference. The inhomogeneity of the interference pattern is caused by the finiteness of the plane waves because of the limitation of the simulation space.

3. Sidelobe suppression

In order to preserve the central fringe only, a square aperture is used to suppress the sidelobes. A metal film with an aperture of side D in its centre is located on the interface, which is taken as a perfect electric conductor (PEC) with infinite conductivity. In the near-field zone of the interface, the strength of the $k_{\|}$ components of the $\boldsymbol{k}$ wave vectors ranges from zero to $k_{\|\max}$. From the near-field scattering relation, the evanescent field decay is directly related to the strength of the $k_{\|}$ vector. The observation distance plays the role of a spatial low-pass filter for the electromagnetic field. This will result in a broadening of the light confinement zone when the observation plane leaves the piece of material generating the field distribution.

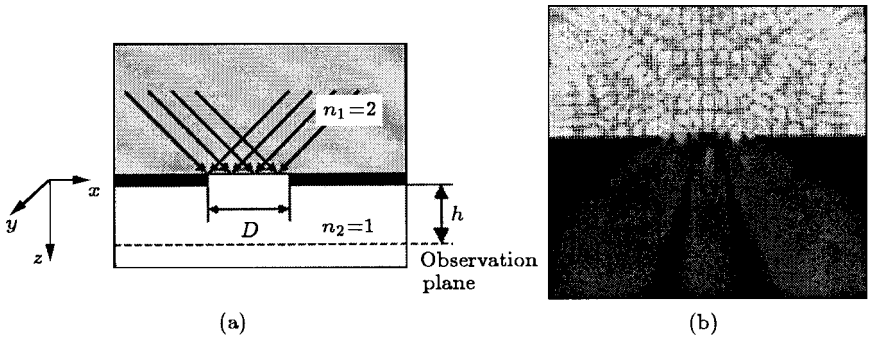


Fig.4. (a) Square aperture diffraction simulation model. (b) The steady-state electric field distribution in the xz plane.

The simulation model has been built up for understanding the diffraction effect of the small aperture. Figure 4 shows the simulation model and the steady-state electric field distribution in the xz section. The centre of the aperture and the origin of the Cartesian coordinate are defined as the centre of the interface.

The intensity distribution on the observation plane of the simulation model and the x section distribution in Fig.4 are shown in Fig.5, where h is 250nm and the side length of aperture is 1.5μm. The size of the section view is 5μm and the FWHM of the central peak is about 230nm. As expected, on the observation plane there is a symmetrical distribution with a sharp peak and the sidelobes are suppressed effectively. The distribution is axially symmetric of y and the y component of distribution is dominant, which is related to the polarization of incident light. One can assume that a centrosymmetric distribution can be achieved if the incident light is an annular beam with circular polarization and the aperture is round based on the principle of symmetry. The centrosymmetric light intensity peak is the effective part of the virtual probe.

According to the simulation results, the virtual probe has an effect on the condition of evanescent wave interference and the light confinement by an aperture, as shown in Fig.4(a). Further simulations based on this model are carried out to investigate the characteristics of the virtual probe such as the transmission efficiency, width and depth. The influence of the aperture size is considered.

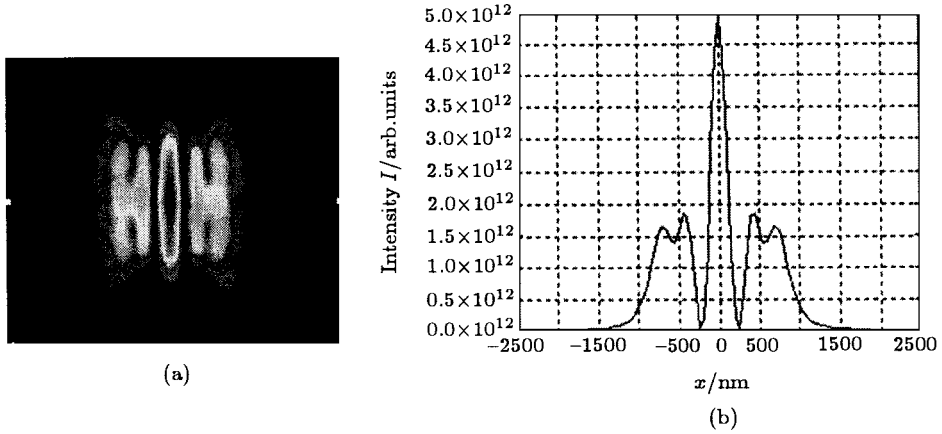


Fig.5. (a) Intensity distribution and (b) section along the x-direction on the observation plane (h=250nm, D=1.5μm).

As shown in Fig.6 the transmission efficiency has almost a linear relation with the size of aperture whose order of magnitude is about 10^{-2}, which is about 10^2–10^4 times higher than a usual nano-aperture probe used in near-field optical technology.

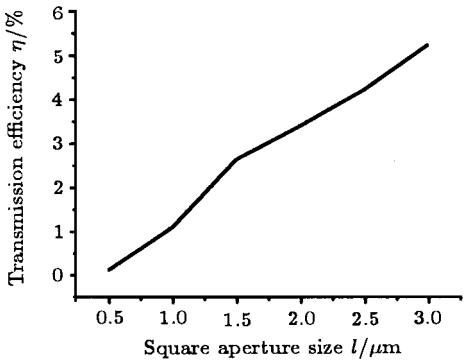


Fig.6. Transmission efficiency versus aperture size.

Figure 7 shows that the FWHM of central peak (about 300nm) is constant whatever the distance z in the range of 500 nm. When the side lengths of aperture are 3 and 1.5μm, the FWHM remains constant in ranges 100–650 and 100–600nm, respectively, which shows the effective depth of the virtual probe. When the side length is 0.5μm, the FWHM increases quickly with the distance z, therefore the effect of the virtual probe is not obvious.

The maximum of the peak is at a position of 200nm away from interface when the side length of the aperture is 1.5μm (see Fig.8). Then the peak intensity decreases with the distance, but the insignificant decrease of about 25–30% of the maximum in the range of 100–400nm is acceptable.

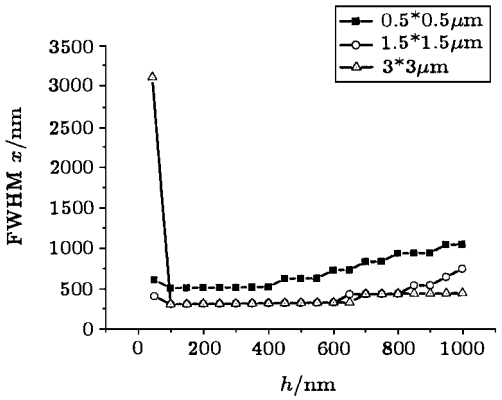


Fig.7. FWHM of central peak versus distance.

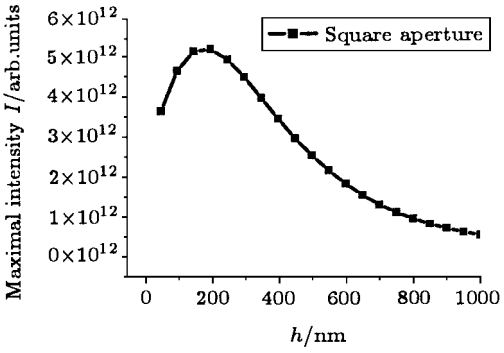


Fig.8. Central peak intensity versus distance.

The evanescent interference effect of the virtual probe is not obvious when the aperture size is smaller than 0.5μm, and the diffraction effect is remarkable. With the increase of aperture size, the evanescent interference effect becomes notable gradually, and a sharp peak emerges at the centre of the field distribution and the sidelobes are so small as to be ignored. But when the aperture size is greater than 3μm, many sidelobes appear, which is not good for the application of the virtual probe.

4. Application prospect of the virtual probe

The novel virtual probe can be used in near-field high-density optical data storage, nano-lithography, near-field optical imaging and spectral detection, near-field optical manipulation of nano-scale specimen, etc. In this section, we give a design example of the application of the virtual probe in ultrahigh-density optical data storage.

One way to realize near-field recording is solid immersion lens (SIL) near-field optical storage. The size of the recording laser spot is decreased by utilizing the SIL with a high refractive index. If the recording media is placed close enough to the flat surface of the SIL, this subwavelength spot size is obtained at the media and the optical energy is transferred into the media through near-field coupling. In this case, the effective numerical aperture of the lens can be greater than one. Although the SIL method can get a much higher transmission efficiency than the probe and higher resolution than the traditional objective, it is very difficult to keep the distance between the SIL and the recording media in the near-field region (about 50nm). Thus, the SIL or recording media may be easily damaged by scratches or dust.

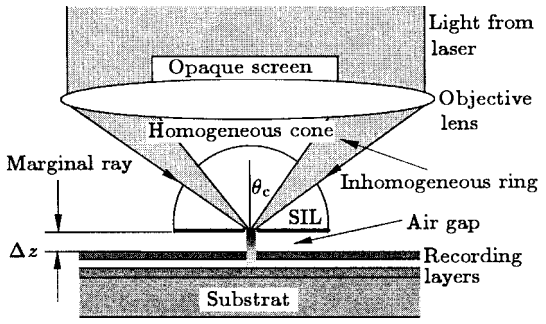


Fig.9. Proposed layout of the virtual probe used in the optical data storage system.

The concept of the virtual probe can be applied to SIL near-field optical storage to ensure that the FWHM of light distribution does not change with distance in a certain range so that the rigorous distance control can be relaxed and the damage of recording head or media can be avoided. This will be very important for the development of near-field optical storage.

A detailed view of the proposed virtual probe in the SIL system is shown in Fig.9. A laser beam is focused by an objective lens on the bottom plane surface of the SIL, on which a metal film is coated with an aperture in the centre. The recording material and the SIL are separated by an air gap of thickness Δz. The incident light on the SIL/air interface can be divided into a homogeneous cone for angles smaller than θ_c and an inhomogeneous ring for angles larger than θ_c. The homogeneous cone is blocked by an opaque screen and the inhomogeneous ring is focused on the plane surface. The virtual probe is formed in the gap by evanescent wave interference and small aperture diffraction. In fact, the light distribution is similar to that from a hole-type aperture, but the light intensity is 100 times larger than that of a fibre probe.

In the traditional near-field optical storage system, including both the hole-type probe and SIL system, the recording layer must be in proximity to the coupling surface (50nm). Without close proximity, the spot size increases and the total energy available for coupling into the recording layer decreases due to evanescent decay. What differentiate the traditional near-field system from the virtual probe are the separation control and the transmission efficiency. The characteristic that virtual probe light distribution does not change with distance in a certain range (about 100–500nm) makes the separation control simple and the collision between the recording head and media can be avoided. The problem of low throughput power in probe-type near-field optical storage also can be solved utilizing the virtual probe.

5. Conclusions

The virtual probe based on evanescent wave interference and small aperture has a transmission efficiency of 10^2–10^4 times larger than an ordinary nano-aperture probe used in the near-field optical system. The FWHM of the central peak of the virtual probe remains constant whatever the distance in a certain range. It is possible that the interaction volume is beyond the diffraction limit and the interaction distance is ten times larger than the ordinary near-field distance owing to its characteristics. The distribution of the virtual probe could be influenced by the shape and size of the aperture, polarization of incident light, etc. The parameter optimization of the aperture, incident angle, the refractive index, etc, is an important issue to be studied further. The characteristics of the virtual probe will make it possible to use it in near-field optical storage systems, nano-lithography, near-field imaging and spectrum detection, and in the near-field optical manipulation of nano-specimens.

Acknowledgment

The authors would like to thank Professor Min Gu (Swinburne University of Technology, Australia) for a helpful discussion.

References

[1] Betzig E and Trautman J K 1992 *Science* **257** 189
[2] Weeber J C, Bourillot E, Dereux A *et al* 1996 *Phys. Rev. Lett.* **77** 5232
[3] Girard C, Dereux A, Matin O *et al* 1995 *Phys. Rev.* B **52** 2889
[4] Sun L Q, Zhang Y P, Liu Y F *et al* 2000 *Acta Phys. Sin.* **49** 724 (in Chinese)
[5] Greffet J J and Carminati R 1997 *Prog. Surf. Sci.* **56** 133
[6] Grosjean T and Courjon D 2001 *J. Microscopy* **202** 273
[7] Milster T D 2000 *Proc. IEEE* **88** 1480
[8] Born M and Wolf E 1980 *Principles of Optics* 6th edn (Oxford: Pergamon) p47
[9] Kunz K and Lubbers R J 1993 *The Finite Difference Time Domain Method for Electromagnetics* (New York: CRC Press) p11
[10] Nakamura H, Sawada K, Kamble H *et al* 2000 *Prog. Theor. Phys.* **138** 173
[11] Furukawa H and Kawata S 1996 *Opt. Commun.* **132** 170
[12] Wang C Q and Zhu X L 1994 *The Finite Difference Time Domain Method in Electromagnetic Field Calculation* (Beijing: Peking University Press) p30 (in Chinese)